

Electronic Supplementary Material (ESI) for Nanoscale  
This journal is © The Royal Society of Chemistry 2021

## Electronic Supplementary Information

### Magnetic Liquid Metal Loaded Nano-in-Micro Spheres as Fully Flexible Theranostics for SMART Embolization

Dawei Wang,<sup>ab</sup> Qirun Wu,<sup>c\*</sup> Rui Guo,<sup>d</sup> Chennan Lu,<sup>ab</sup> Meng Niu,<sup>e\*</sup> Wei Rao,<sup>ab\*</sup>

<sup>a</sup> *Technical Institute of Physics and Chemistry, Chinese Academy of Sciences, Beijing 100190, China*

<sup>b</sup> *School of Future Technology, University of Chinese Academy of Sciences, Beijing 100049, China*

<sup>c</sup> *Department of Interventional Medical, Zhuhai People's Hospital (Zhuhai hospital affiliated with Jinan University), Zhuhai 519000, China*

<sup>d</sup> *Department of Biomedical Engineering, School of Medicine, Tsinghua University, Beijing 100084, China*

<sup>e</sup> *Department of Radiology, First Hospital of China Medical University, Shenyang 110001, China*

*\* Corresponding author. E-mail address: weirao@mail.ipc.ac.cn*

## Abbreviations

CA: calcium alginate; EGaIn: Eutectic gallium-indium; Fe@EGaIn: EGaIn containing iron nanoparticles; NPs: nanoparticles; Fe@EGaIn/CA: calcium alginate microspheres loaded with Fe@EGaIn NPs.

## Supplementary Figures

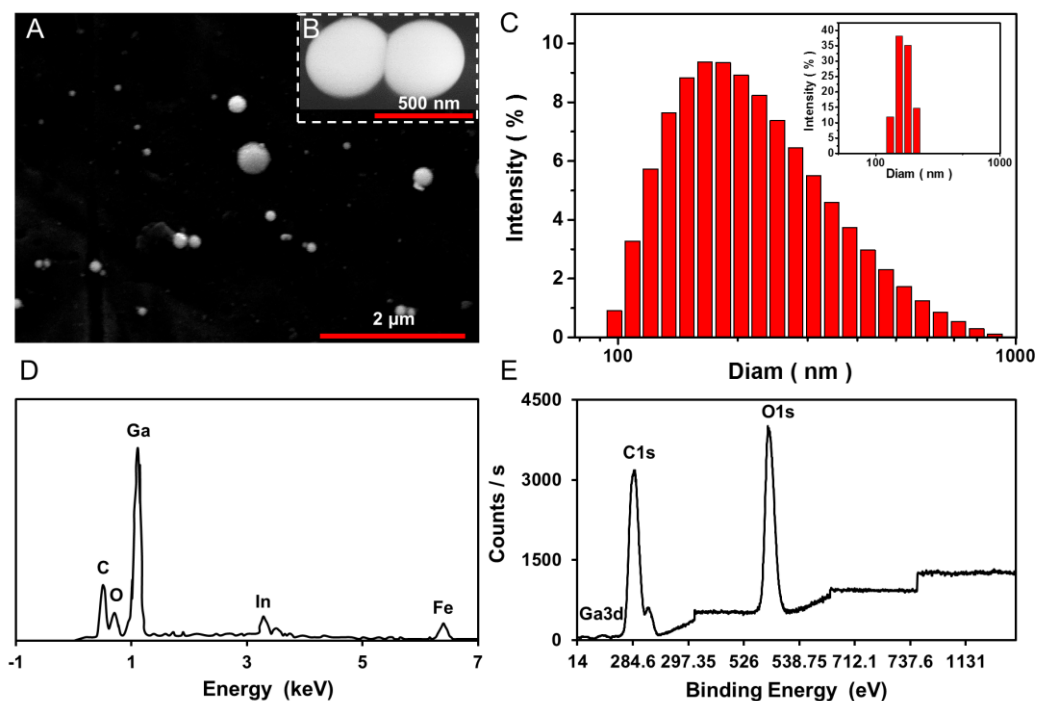


**Fig. S1** Characterization of Fe@EGaIn nanoparticles. (A, B) SEM images of Fe@EGaIn NPs. (C) Particle size statistics of Fe@EGaIn NPs, the inset shows particle size statistics after filtration using a membrane filter (0.45 μm). (D) EDS elemental analysis of Fe@EGaIn NPs. (E) XPS spectra of Fe@EGaIn NPs.

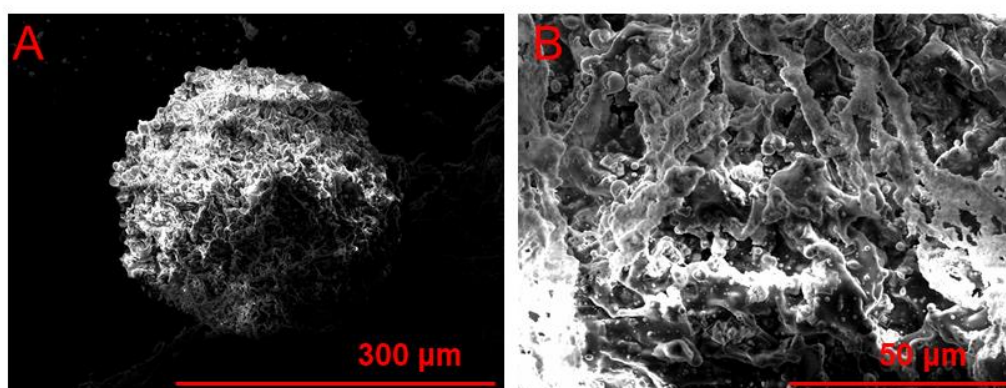


**Fig. S2:** (A-B): SEM images of the morphology of the ALG/EGaIn@Fe NPs microsphere after freeze-drying, showing the porous network structure.

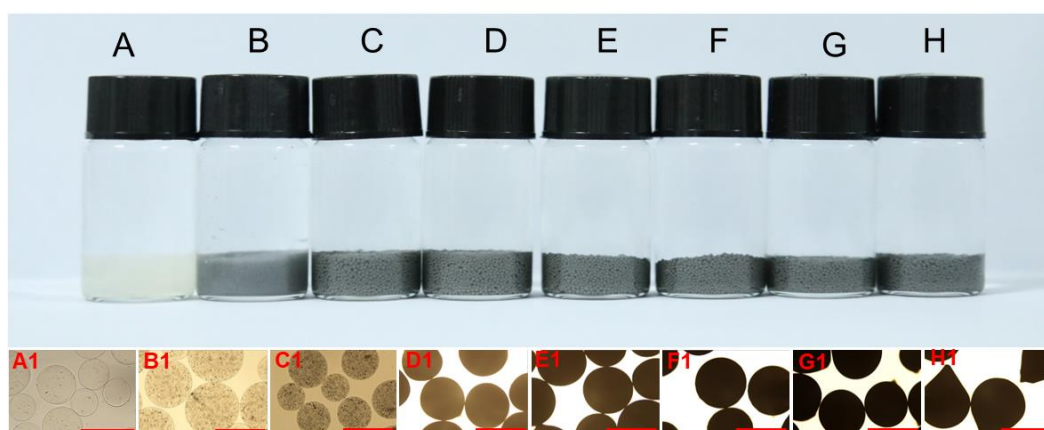


**Fig. S3** Optical photographs (A-H) and optical micrographs (A1-H1) of the morphology of the Fe@EGaIn/CA microspheres encapsulated with varied concentrations of Fe@EGaIn NPs, scale bars: 500  $\mu\text{m}$ .

**Notes** (A, A1) 0; (B, B1) 2.5; (C, C1) 5; (D, D1) 10; (E, E1) 25; (F, F1) 50; (G, G1) 100; (H, H1) 200 mg/mL.

**Table S1** Characterization of Fe@EGaIn/CA microspheres

Content of Fe@EGaIn NPs (mg/mL)	10	25	50	100
Average Diameter ( $\mu\text{m}$ )	$518.8 \pm 54.8$	$526.3 \pm 50.7$	$494.2 \pm 65.4$	$483.8 \pm 48.6$

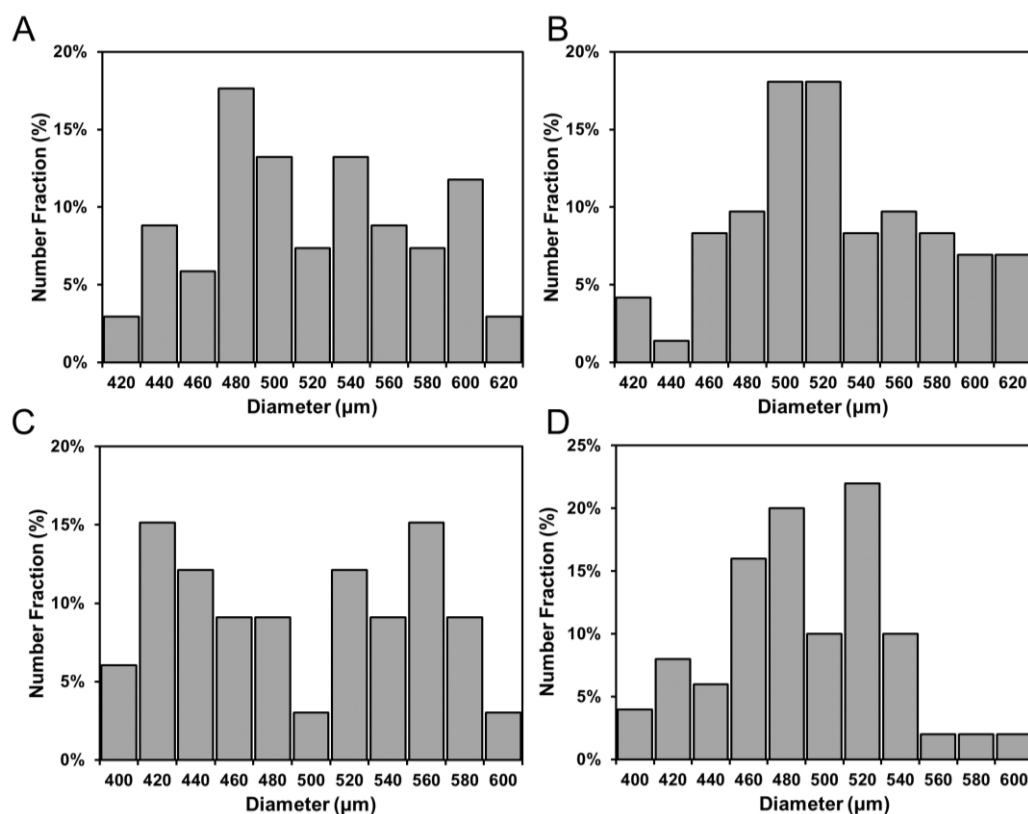


**Fig. S4** Corresponding size distribution histogram of the Fe@EGaln/CA microspheres encapsulated with varied contents of Fe@EGaln NPs. (A) 10; (B) 25; (C) 50; (D) 100 mg/mL.

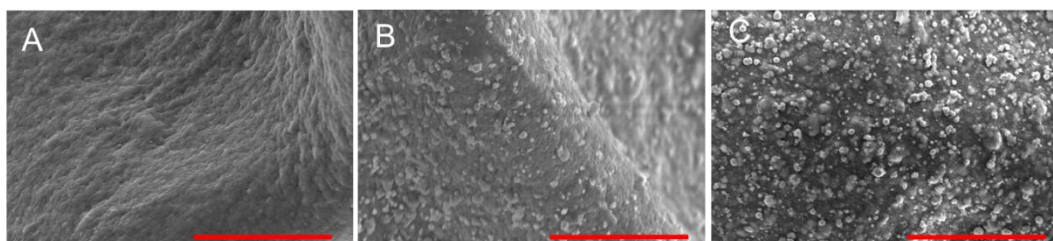


**Fig. S5** (A-C) Enlarged SEM image of the surface of one Fe@EGaln/CA microsphere containing 0, 5, and 25 mg/mL Fe@EGaln NPs, scale bars: 20 μm.

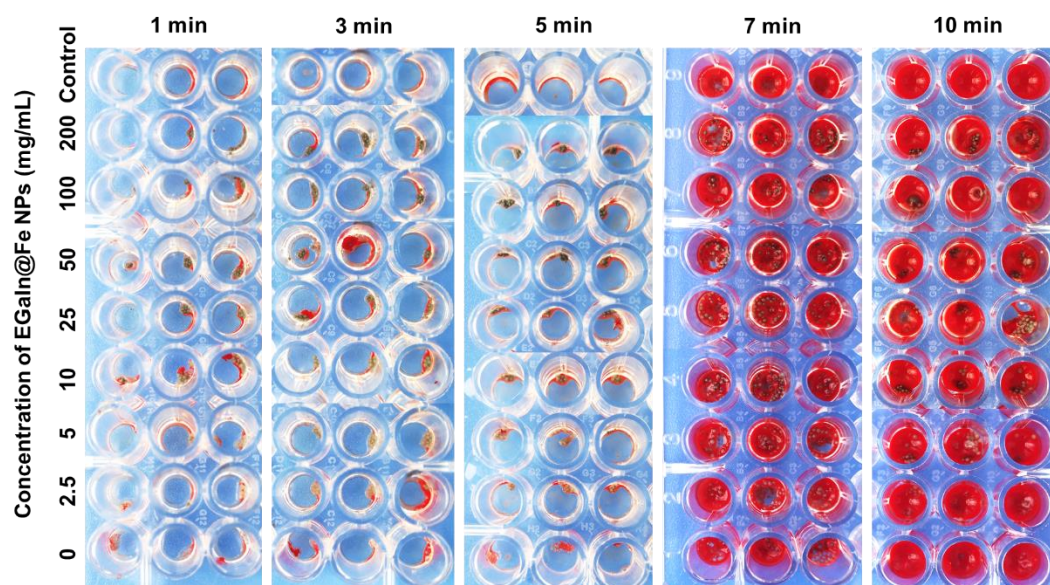


**Fig. S6** Plate assay (96-well) of blood clotting in contact with the Fe@EGaIn/CA microspheres (containing various concentrations of Fe@EGaIn NPs) and controls (blank wells with citrated blood), each group had three parallel.

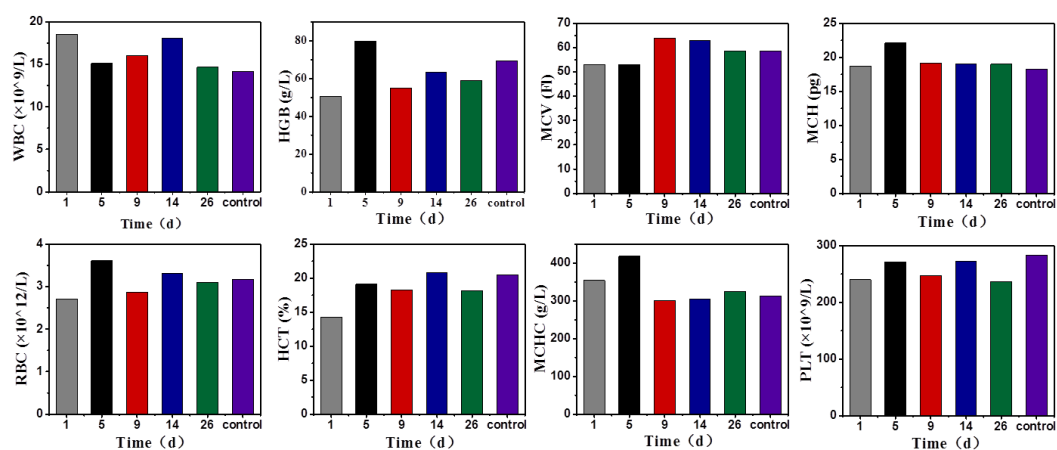


**Fig. S7** The blood test results (day 1, 5, 9, 14, and 26) after embolization at the pig's liver with Fe@EGaIn/CA microspheres.





**Fig. S8** The implantation of VX2 cells and the process of tumor growth, scale bars: 2 cm.

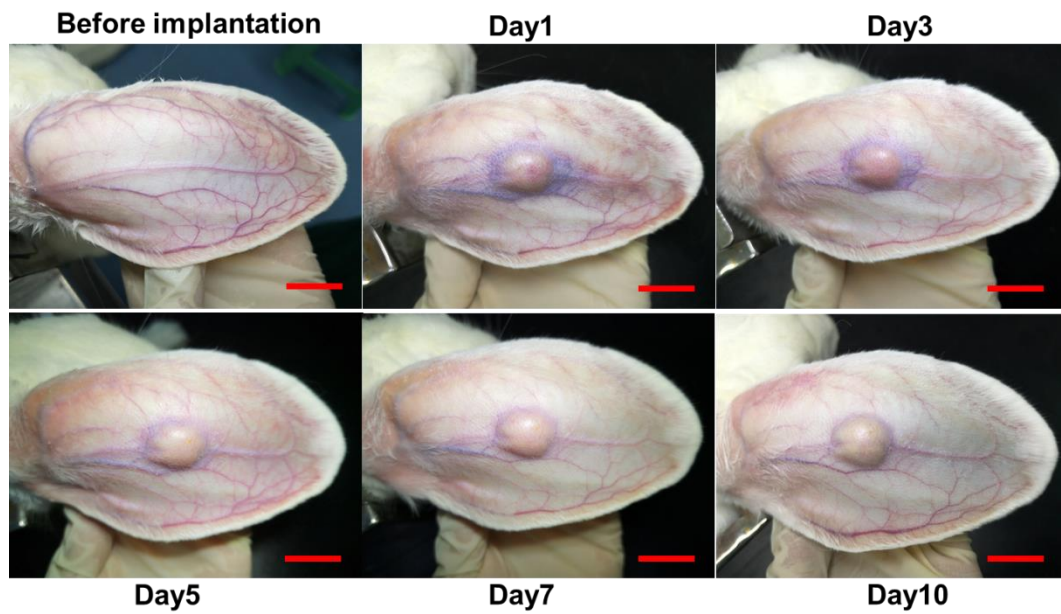


**Fig. S9** Tumor growth in the blank group during embolotherapy, scale bars: 2 cm.

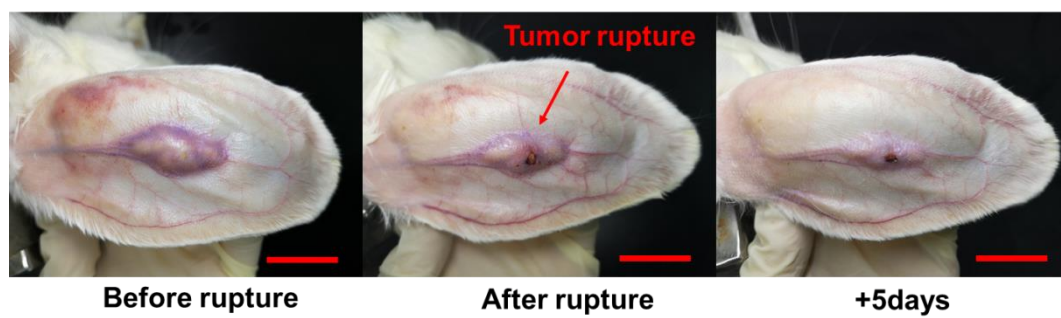


**Fig. S10** Tumor rupture in the blank group during embolotherapy, scale bars: 2 cm.

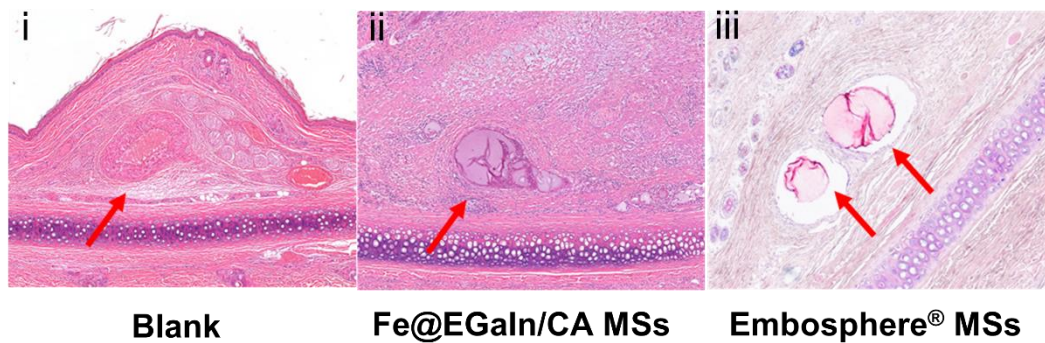


**Fig. S11** Microscopic images of HE stained histological sections of ears with or without embolization; (arrows: artery untreated (i) and arteries embolized with Fe@EGaIn/CA microspheres (ii, ~500  $\mu\text{m}$ ) or Embosphere® microspheres (iii, 300~500  $\mu\text{m}$ )); The magnification:  $\times 50$ , scale bars: 200  $\mu\text{m}$ ;

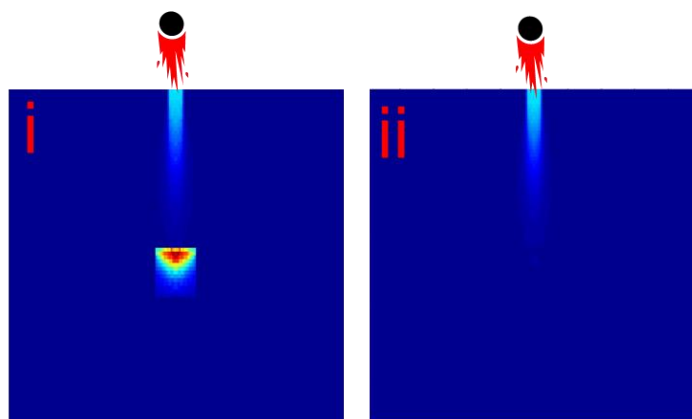


**Fig. S12** The 2D NIR laser energy distribution profile obtained by numerical simulation using Matlab software, (i) With Fe@EGaIn NPs, (ii) Without Fe@EGaIn NPs; A higher laser energy density was observed in the central tumor area, because the Fe@EGaIn NPs enhanced the NIR laser absorption of cancerous tissues, thereby effectively improving the photothermal conversion effect and increasing the photothermal penetration depth.

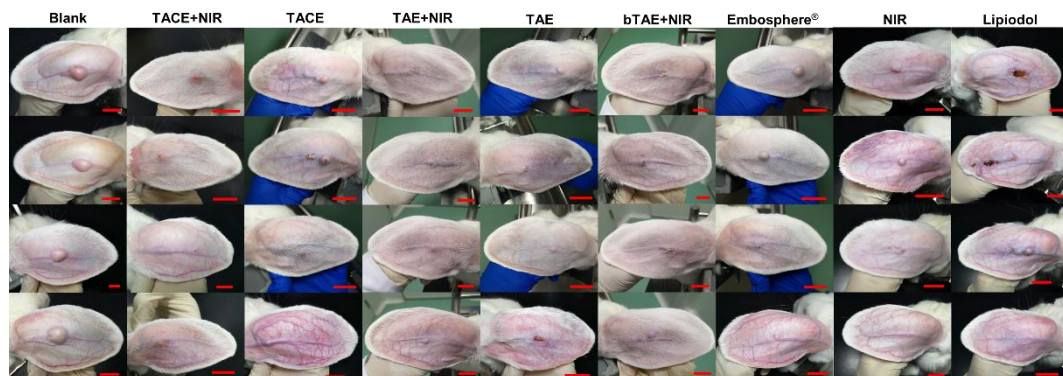


**Fig. S13** Representative photographs of auricle tumor-bearing rabbits' ears in each group after treatment, showing the tumors' sizes at the end of observation (Day 10 in Blank group and Day 21 in other groups), scale bars: 2 cm.

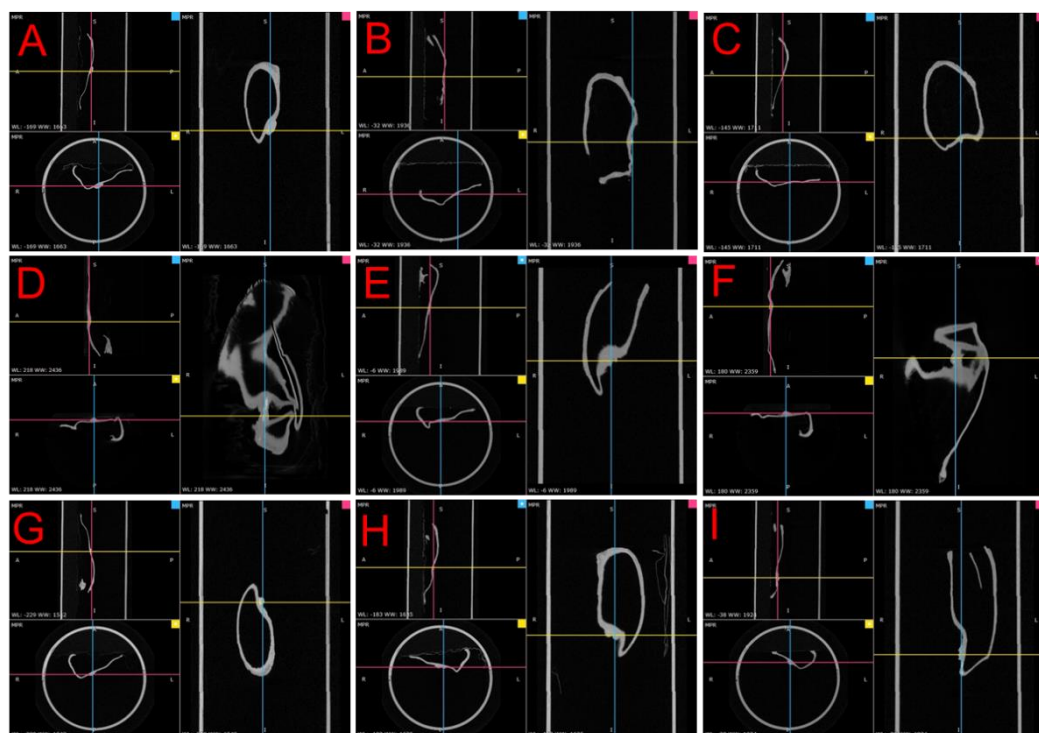


**Fig. S14** CT images of the auricle tumor-bearing rabbits' ears after treatment. (A) Blank group, (B) TACE+NIR group (C) TACE group (D) TAE+NIR group (E) TAE group (F) bTAE+NIR group (G) Embosphere® group (H) NIR group (I) Lipiodol group.



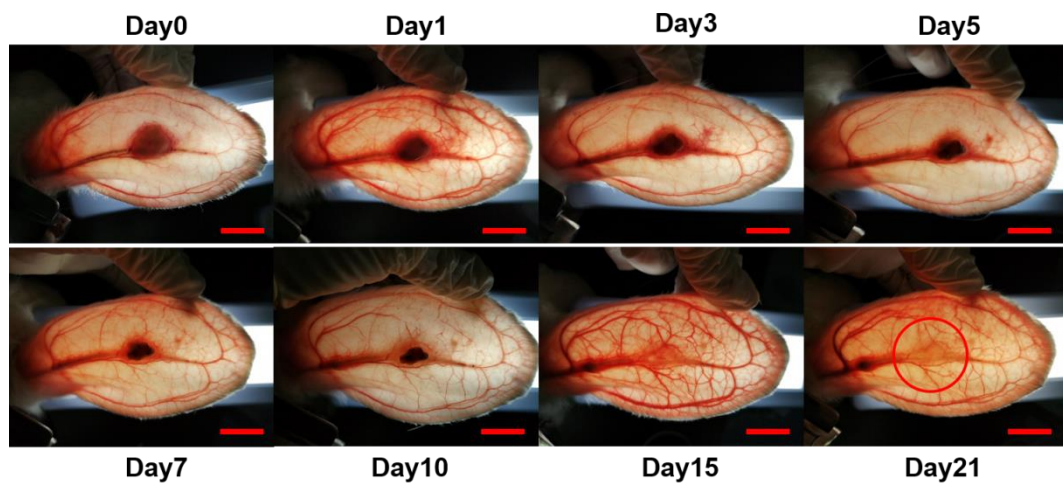


**Fig. S15** The process of tumor disappearing during the embolization using Fe@EGaln/CA microspheres, showing that tissue around the embolization site maintains a normal state and the tumor became ischemic necrosis and gradually disappeared without visible damage to normal tissue (red circle); scale bars: 2 cm.

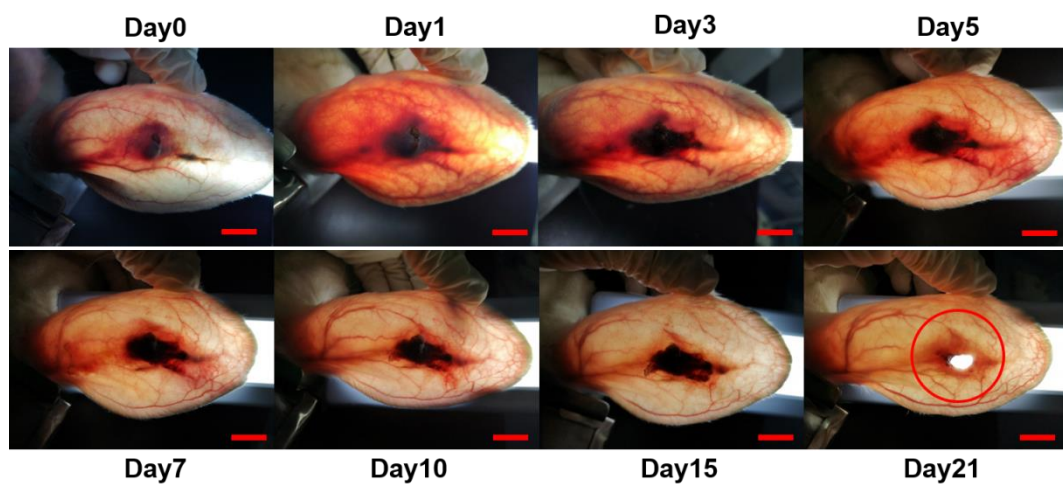


**Fig. S16** The process of tumor disappearing during the embolization using lipiodol, showing that there was significant redness and swelling around the embolization site and eventually cause severe damage to normal tissues (red circle); scale bars: 2 cm.

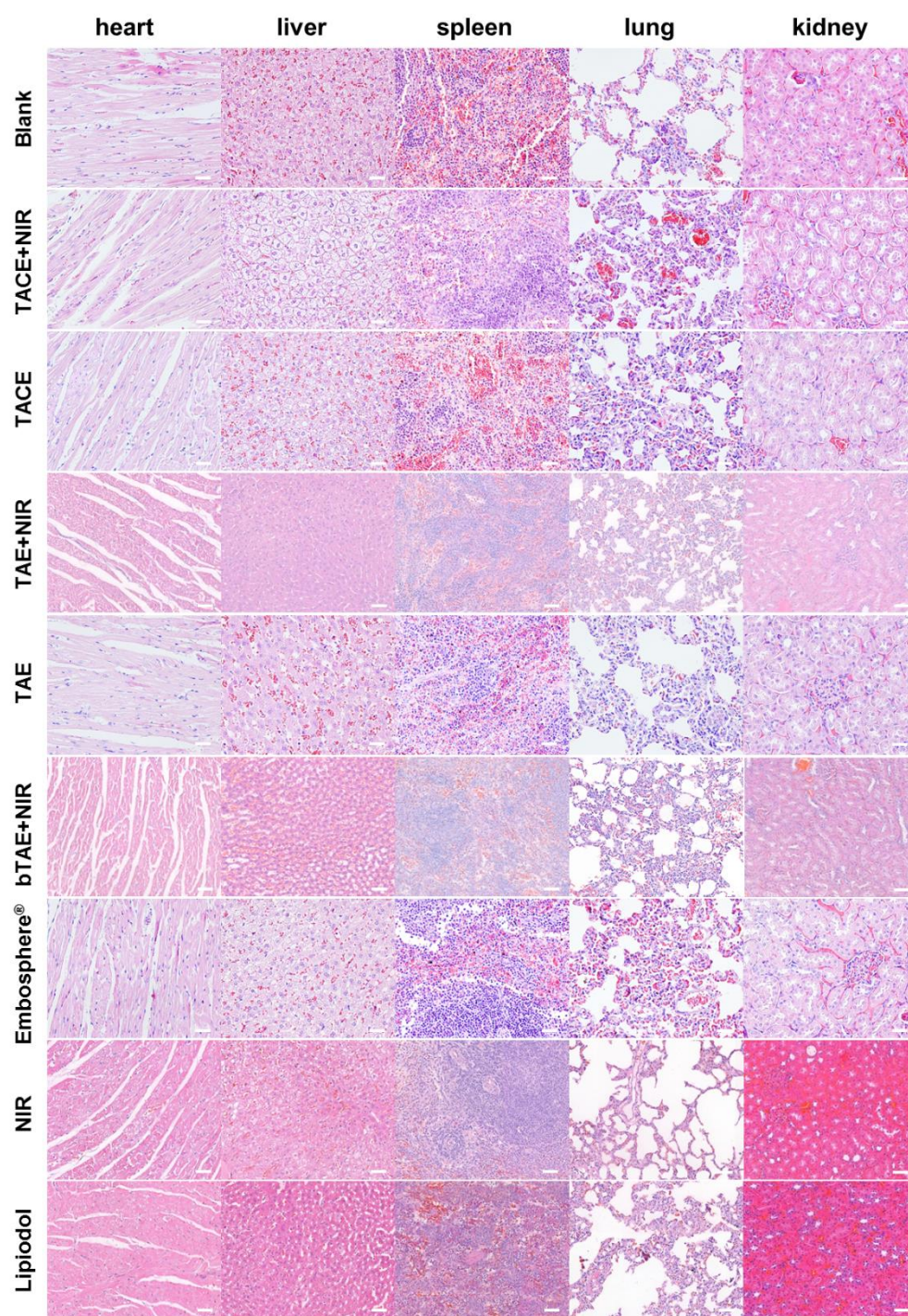


**Fig. S17** Microscopic images of HE stained histological sections of the heart, liver, spleen, lung, and kidney in each group after treatment. The magnification:  $\times 200$ , scale bars: 50  $\mu\text{m}$ .



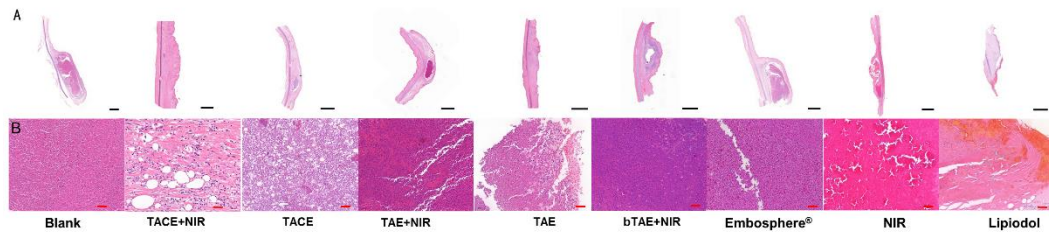


**Fig. S18** Microscopic images of HE stained histological sections of the tumor. (A) the magnification:  $\times 5$ , scale bars: 2000  $\mu\text{m}$ ; (B) the magnification:  $\times 200$ , scale bars: 50  $\mu\text{m}$ .

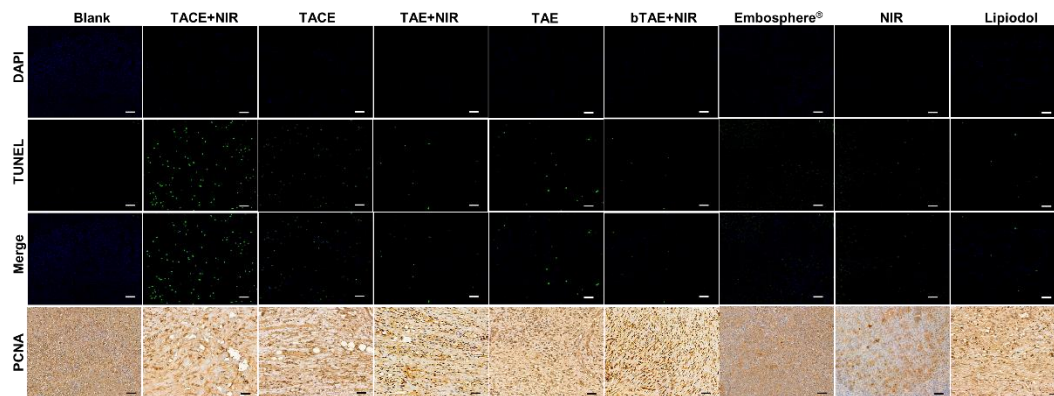


**Fig. S19** The expression of DAPI, TUNEL, and PCNA in tumor tissue of each group by immunofluorescence and immunohistochemical examination. The nucleus appearing fluorescent blue was for DAPI-positive cells and the fluorescent green represents TUNEL-positive cells; The nucleus appearing brown was for PCNA-positive cells, and the blue represents the negative cells; The magnification:  $\times 200$ , scale bars: 50  $\mu\text{m}$ .

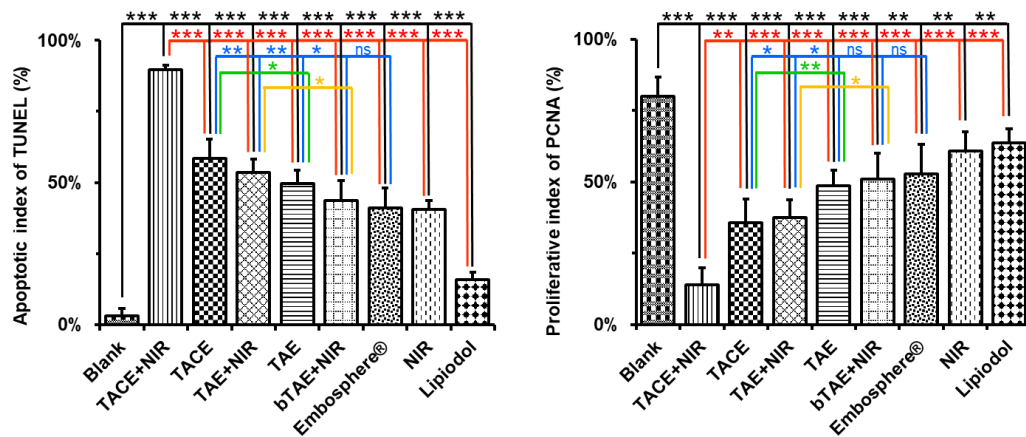


**Fig. S20** The apoptotic index (AI) of TUNEL and the proliferative index (PI) of PCNA in each group, showing that the Blank group had lower AI and higher PI than other groups (black line), the TACE+NIR group had significantly higher AI and lower PI than that of the other groups (red line), and there were also obvious difference between TACE group and TAE group (green line) or Embosphere® group (blue line); ns  $p > 0.05$ ; \* $p < 0.05$ ; \*\* $p < 0.01$ ; \*\*\* $p < 0.001$ .

#### Movie S1

Animation illustration of NIR laser enhanced transarterial chemoembolization using Fe@EGaIn/CA microspheres.

#### Movie S2

Embolization of pig liver artery using Fe@EGaIn/CA microspheres.

#### Movie S3

Embolization of rabbit liver tumor feeding artery using Fe@EGaIn/CA microspheres.

#### Movie S4

The 3D reconstructed CT images of the ears after treatment. Central artery embolized with blank calcium alginate microspheres or Fe@EGaIn/CA microspheres.

#### Movie S5

The 3D reconstructed MR images of the ears after treatment. Central artery embolized with blank calcium alginate microspheres or Fe@EGaIn/CA microspheres.